

# REVIEW OF CMS AND TOTEM RESULTS ON MULTI-PARTON INTERACTIONS, SOFT QCD AND DIFFRACTION\*

GRZEGORZ BRONA

for CMS and TOTEM collaborations

University of Warsaw, Faculty of Physics, 00-681 Warszawa, Poland

*(Received November 12, 2015)*

CMS results on the multiple parton interactions measured with the leading track and the leading charged particle jet in  $pp$  collisions at different  $\sqrt{s}$  are presented. The charged particles distributions in central CMS detector and in TOTEM in inclusive sample and sample enhanced with non-diffractive interactions are shown. The single and double diffractive dissociation results are discussed. Finally, the double diffractive cross section measurement in the forward region done by TOTEM is presented.

DOI:10.5506/APhysPolBSupp.8.763

PACS numbers: 12.38.Qk

## 1. Introduction

The hard QCD process in  $pp$  interaction is accompanied by an additional hadronic activity, an underlying event (UE). The UE is a sum of multiple parton interactions (MPI), initial and final state radiation (ISR, FSR) and beam-beam remnants. As UE involves soft QCD, it cannot be computed from the first principles and has to be described by phenomenological models tuned with the input from measurements. One of these, is an analysis in which in each event, a direction of a leading object (track or jet with the largest  $p_T$ ) is defined. Then, the  $\eta$ - $\phi$  plane is divided into 3 regions with respect to the azimuthal angle of the leading object. These are: toward ( $\Delta\phi < 60^\circ$ ), away ( $\Delta\phi > 120^\circ$ ) and transverse ( $60^\circ < \Delta\phi < 120^\circ$ ) regions. In these regions, the charge density  $N_{\text{ch}}$  and the scalar sum of the transverse momentum density  $\sum p_T$  are calculated. These quantities are plotted as functions of the hard scale of an event set by the  $p_T$  of a leading object. The second approach to the UE activity measurement is an analysis of the

---

\* Presented at EDS Blois 2015: The 16<sup>th</sup> Conference on Elastic and Diffractive Scattering, Borgo, Corsica, France, June 29–July 4, 2015.

charged particles distribution as a function of  $\eta$ . To minimize the diffractive component, the data are, in addition to the inclusive sample, selected with a requirement of tracks reconstructed in both TOTEM T2 telescopes ( $5.3 < |\eta| < 6.5$ ). Indeed, an additional factor to be considered in UE studies is the unknown contribution from the diffractive interactions. In CMS, this contribution is studied in a separate analysis [1]. The diffractive interactions account for about 25% of the total inelastic  $pp$  cross section. They are mediated by a color-singlet object carrying vacuum quantum numbers, called Pomeron. The signature of the diffraction is an appearance of at least one large rapidity gap (LRG) in the final state, experimentally detected as a region in pseudorapidity without any activity. There are three main types of diffractive processes. (i) Single dissociation (SD) in which one of the proton taking part in the interaction dissociates and the second stays intact. The process is characterized by an existence of a LRG at the one side of the detector, while the other side, if only the diffractive mass is large enough, is populated by particles from the dissociation. (ii) Double dissociation (DD) when both protons dissociate and the LRG is located between the two areas populated by the particles. (iii) Central diffraction (CD) which technically is a Pomeron–Pomeron interaction and is leading to the creation of the central system separated from the two intact protons by two LRGs. This last contribution is negligible. The double diffraction is also studied by TOTEM with tracking detectors T1 and T2 [2]. This gives an access to the diffractive systems within  $4.7 < |\eta|_{\min} < 6.5$ , where  $\eta_{\min}$  is the minimum pseudorapidity of all primary particles produced in the system.

## 2. Measurement of the UE activity using leading objects and measurement of the charged particles distribution

The analysis using leading tracks is performed with the 2010 low pile-up data at  $\sqrt{s}$  of 0.9 and 7 TeV [3]. Events are selected with a minimum bias trigger based on an activity at both sides of CMS recorded in Beam Scintillator Counters [4]. Offline, events with only one vertex are selected. Tracks used to calculate the observables are required to have  $p_T > 0.5$  GeV and be contained within  $|\eta| < 0.8$  region. In Fig. 1, both observables are plotted. Below  $p_T$  of 5 GeV, a rapid rise of MPI activity is observed. This corresponds to a selection of more central collisions with a cut on the energy scale set by a leading track. At some scale, the collisions cannot be more central and an increase is much slower. It corresponds to the raise of the UE activity due to the radiative contributions, energy scale, and harder fragmentation. The data are compared to Monte Carlo predictions. The best agreement is obtained for PYTHIA6-Z1 tune. A track jet with a highest  $p_T$  is used as a leading object in the second analysis [5]. Selecting leading jets provides an access to much higher scales and decreases sensitivity to

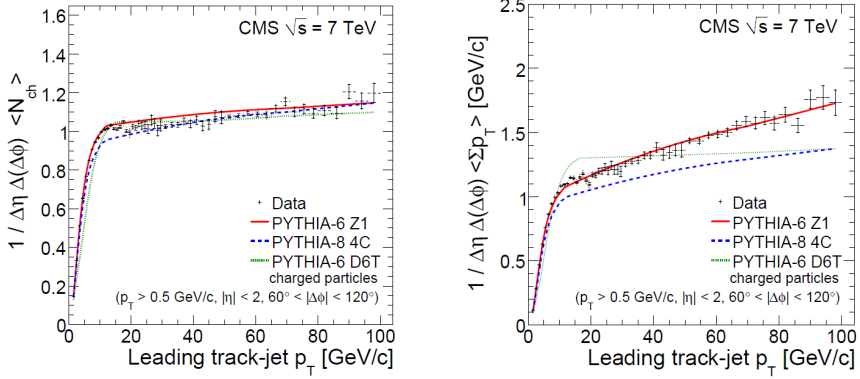


Fig. 1. The average multiplicity (left) and the average scalar  $\sum p_T$  (right) for 7 TeV for the leading track analysis.

the hadronization and shower effects. The transverse region is divided into two opposite in  $\phi$  subregions: transMin with a lower activity and transMax. The former is sensitive to the MPI and beam–beam remnants, while the latter to MPI, beam–beam remnants and ISR and FSR. The analysis includes 2.76 TeV data with a negligible pile-up. The tracks are required to have  $p_T > 0.5$  GeV and be inside  $|\eta| < 2.0$  region. In transMax, a slow rise at larger  $p_T$  is observed, while in transMin, a wide plateau is present

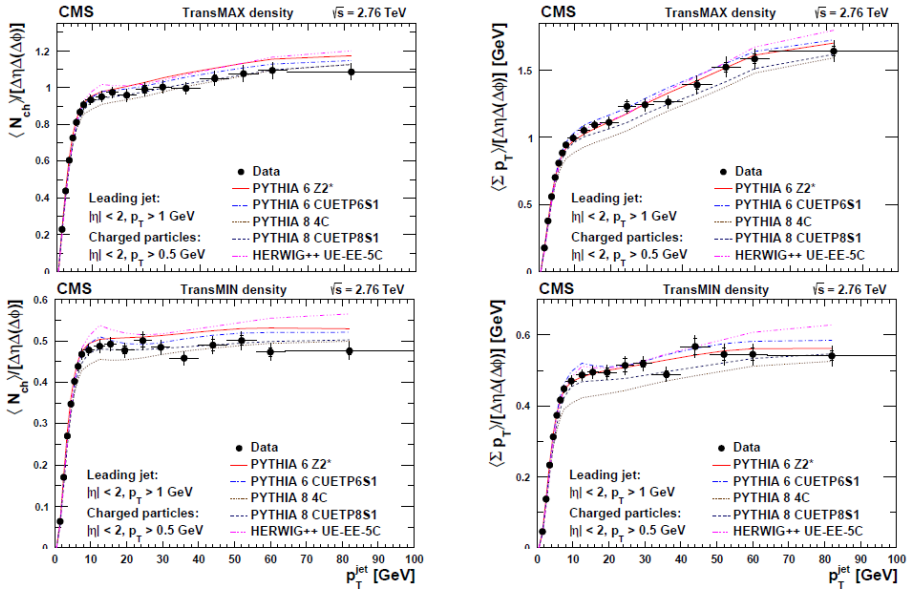


Fig. 2. The average multiplicity (left) and the average scalar  $\sum p_T$  (right) for 2.76 TeV leading jet analysis for transMax (top) and transMin (bottom) regions.

(see Fig. 2). The conclusion is that the MPI and beam–beam remnants are almost independent on the hard scale once the most central events are selected, while the ISR and FSR increase with  $p_T$ .

The charged particles distribution as a function of  $\eta$  is obtained for 8 TeV data sample. The trigger is provided by an activity in TOTEM T2 telescopes which corresponds to the presence of tracks in  $5.3 < |\eta| < 6.5$  region with  $p_T > 40$  MeV. In the inclusive sample, there are events with signal in at least one T2, while the non-single diffractive enhanced (NSDE) sample requires activity at both sides of CMS. The distributions are obtained for both samples for tracks with  $p_T > 0.1$  GeV and then extrapolated to  $p_T = 0$  with PYTHIA predictions. They are presented in Fig. 3 together with predictions from MC. The best description is obtained by QGSJETII-04. For more details see [6].

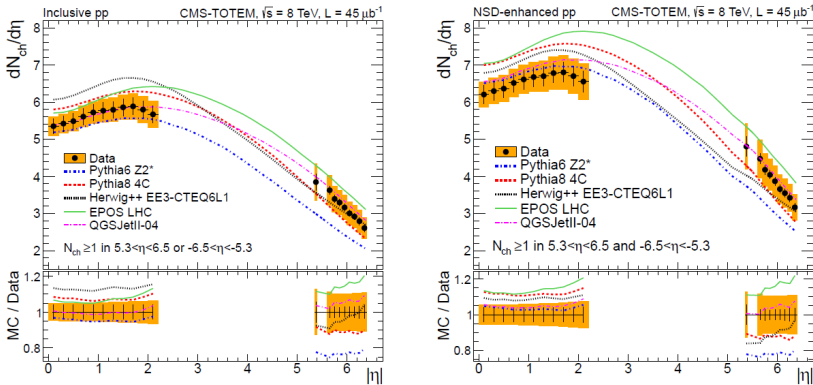


Fig. 3. Charged particle pseudorapidity distribution for inclusive sample (left) and non-single diffractive enhanced sample (right).

### 3. Soft diffraction

The soft diffraction analysis is based on the  $\sqrt{s} = 7$  TeV data. The integrated luminosity of  $16.2 \mu\text{b}^{-1}$  with an average of  $\mu = 0.14$  inelastic  $pp$  collisions per bunch crossing is used. The events are selected with minimum bias trigger with the offline requirement on at least two particles reconstructed within the BSC acceptance. To correct data to hadron level input from PYTHIA8-MBR model is used. The model is based on a renormalized Regge theory model, unitarized by interpreting the Pomeron flux as the probability for forming a diffractive rapidity gap. The corrected distributions are compared to PYTHIA8-MBR, PYTHIA8-4C, PYTHIA6-Z2\*, PHOJET, QGSJET-II and EPOS LHC. To enhance the SD and DD components subsamples are defined by requiring presence of a LRG. Three subsamples are formed: FG1

sample containing events with a gap at the edge of the detector on the positive  $\eta$  side, FG2 with a gap on the negative  $\eta$  side and CG sample with a central gap located around  $\eta = 0$ . The FG2 topology can be further decomposed into SD-enhanced and DD-enhanced subsamples. This is done looking for a presence of a signal in the CASTOR detector. If a signal is present, an event is included into the CASTOR-tag sample and in the other case into the no-CASTOR-tag sample. The first of these contains then mostly DD events (with  $0.5 < \log_{10}M_Y < 1.1$  GeV, where  $M_Y$  stands for a diffractive mass formed at the negative rapidities), while the second mostly SD events with a small admixture of DD events with a diffractive mass too low to produce signal in CASTOR ( $\log_{10}M_Y < 0.5$  GeV). In both samples, the cross section as a function of  $\xi_X$  defined as  $\xi_X = M_X^2/s$  is measured. The  $\xi_X$  is reconstructed experimentally summing up the energies and longitudinal momenta of all the tracks in an event. In Fig. 4, the unfolded cross sections are compared with MC predictions. The best description in both samples is obtained with PYTHIA8-MBR model with  $\epsilon = 0.08$  (intercept). The CG sample is used to measure a central pseudorapidity gap cross section as a function of its width corrected for the detector effects,  $\Delta\eta^0$ . The quoted cross section corresponds

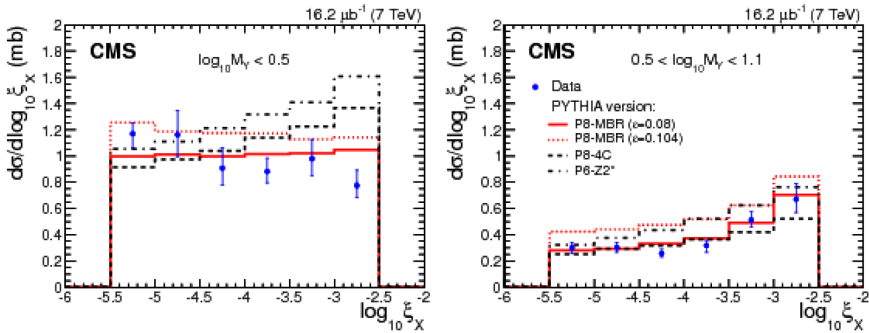


Fig. 4. Cross sections for  $\log_{10}M_Y < 0.5$  no-CASTOR-tag sample (left) and for  $0.5 < \log_{10}M_Y < 1.1$  CASTOR-tag sample (right), comparison with PYTHIA.

to the range of  $\Delta\eta > 3$  and  $\log_{10}M_{X(Y)} > 1.1$  GeV. Again, PYTHIA8-MBR describes the data best (see [1]). From the no-CASTOR-tag sample, the SD cross section corresponding to the  $-5.5 < \log_{10}\xi_X < -2.5$  is calculated. The sample is first corrected for the DD contribution with the MC based correction. The obtained result is  $\sigma^{\text{SDVis}} = 4.06 \pm 0.04(\text{stat.})^{+0.69}_{-0.63}(\text{syst.})$  mb. It corresponds to both  $pp \rightarrow Xp$  and  $pp \rightarrow pY$ . To calculate the visible cross section for the DD events, the following procedure is implemented. First the  $\sigma_{\text{CASTOR-tag}}$  and  $\sigma_{\text{CG}}$  are corrected for the non-diffractive component. This is done using PYTHIA8-MBR and leads to  $\sigma_{\text{CASTOR-tag}}^{\text{DDVis}}$  and to  $\sigma_{\text{CG}}^{\text{DDVis}}$ . Then the  $\sigma^{\text{DDVis}} = 2\sigma_{\text{CASTOR-tag}}^{\text{DDVis}} + \sigma_{\text{CG}}^{\text{DDVis}}$  is evaluated. Fac-

tor 2 assumes the same dependence of the DD cross section on both sides of CMS. The  $\sigma^{\text{DDVis}} = 2.69 \pm 0.04(\text{stat.})_{-0.30}^{+0.29}(\text{syst.})$ . The comparison of the measured cross sections with the results of other experiments and predictions of the theoretical models requires extrapolation of the  $\sigma^{\text{SDVis}}$  to the wider region corresponding to  $\xi < 0.05$ . Similarly, the  $\sigma^{\text{DDVis}}$  has to be extrapolated to  $\Delta\eta > 3$ . The extrapolation is done using PYTHIA8-MBR. The extrapolation uncertainties are obtained by varying the Pomeron trajectory parameters in PYTHIA8-MBR,  $\alpha'$  and  $\epsilon$ . The final results are:  $\sigma^{\text{SD}} = 8.84 \pm 0.08(\text{stat.})_{-1.38}^{+1.49}(\text{syst.})_{-0.37}^{+1.17}(\text{extr.})$  mb, for  $\xi_X < 0.05$  and  $\sigma^{\text{DD}} = 5.17 \pm 0.08(\text{stat.})_{-0.57}^{+0.55}(\text{syst.})_{-0.51}^{+1.62}(\text{extr.})$  mb, for  $\Delta\eta > 3$ .

#### 4. Double diffraction with TOTEM

The approach implemented by TOTEM is almost model-independent. The events are selected only if there is at least one particle in both sides in T2 ( $5.3 < |\eta| < 6.5$ ) and no particles within T1 acceptance ( $3.1 < |\eta| < 4.7$ ). With this selection, corrected for trigger efficiency, pileup, detector effects and neutral particles, the visible cross section is calculated. Finally, it is corrected so that both diffractive systems have  $4.7 < |\eta|_{\text{min}} < 6.5$ . This corresponds to the diffractive mass range of  $3.4 < M < 8$  GeV. The data used in the analysis were taken at  $\sqrt{s} = 7$  during dedicated run with low pileup and special optics. The correction for acceptance, efficiencies, neutral particles, migration and other experimental effects was derived from PYTHIA with an uncertainty taken by a comparison with QGSJET-II and PHOJET. Finally, the cross section for double diffractive dissociation is:  $\sigma_{4.7 < |\eta|_{\text{min}} < 6.5}^{\text{DD}} = 116 \pm 25 \mu\text{b}$ , while PYTHIA predicts 159  $\mu\text{b}$  and PHOJET 101  $\mu\text{b}$ .

This work was supported by the Polish National Science Center, under contract DEC-2012/07/E/ST2/01406.

#### REFERENCES

- [1] CMS Collaboration, CERN-PH-EP-2015-062, submitted to *Phys. Rev. D*.
- [2] TOTEM Collaboration, *Phys. Rev. Lett.* **111**, 262001 (2013).
- [3] CMS Collaboration, *J. High Energy Phys.* **1109**, 109 (2011).
- [4] CMS Collaboration, *JINST* **3**, S08004 (2008).
- [5] CMS Collaboration, *J. High Energy Phys.* **1509**, 137 (2015).
- [6] CMS and TOTEM collaborations, *Eur. Phys. J. C* **74**, 3053 (2014).